LEED investigations on Co(0001): The (2×2)-$(K+2CO)$ overlayer

J. Lahtinen,* K. Kauraala, J. Vaari,† and T. Vaara‡
Laboratory of Physics, Helsinki University of Technology, P.O. Box 1100, 02015 HUT, Finland

P. Kaukasoina and M. Lindroos
Institute of Physics, Tampere University of Technology, P.O. Box 692, 33101 Tampere, Finland
(Received 20 October 2000; published 23 March 2001)

The local adsorption structure of the coadsorption phase of K and CO on Co(0001) has been determined at 160 K using dynamical low-energy electron diffraction. The K atoms in the (2×2) overlayer adopt the on-top sites as in the (2×2)-K structure, but the bond length to the nearest Co atom increases by 0.2 Å to 3.14 ±0.05 Å. The CO molecules are shifted from the on-top sites of the $(\sqrt{3}\times\sqrt{3})R30°$-CO structure to the fcc and hcp three-fold hollow sites. The axis of the CO molecule is perpendicular to the surface. The adsorption induce buckling in the top Co layer, pushing the Co atom beneath the K by 0.27 ± 0.03 Å towards the bulk. The optimum length for the C-O bond is 1.22 ± 0.1 Å and that for the C-Co bond 2.0 ± 0.1 Å. The obtained structure is compared to other known CO+K coadsorption structures on transition metals, as well as to the $(\sqrt{3}\times\sqrt{3})R30°$-CO and (2×2)-K structures on Co(0001).

DOI: 10.1103/PhysRevB.63.155402 PACS number(s): 68.35.Bs, 61.14.Hg

I. INTRODUCTION

The coadsorption of alkali metals (AM) with simple molecules like CO or O_2 form a well-defined playground for studying promotion effects in catalytic systems. The interactions of the adsorbed species with the surface and with each other are of great importance in understanding more complicated systems.

The adsorption of CO is generally assumed to take place via charge donation from the 5σ orbital of CO to the empty states of the substrate, whereby the M-CO bond is formed. The simultaneous back donation from the substrate to the antibonding $2\pi^*$ orbital of CO weakens the C-O bond. On the hand, the charges removed from the 5σ level and donated to the $2\pi^*$ level result in a more uniform distribution of the 1π level which strengthens the C-O bond.[1,2] Potassium adsorption has been shown to facilitate the CO dissociation on Ni surfaces, and this has been explained to take place via charge transfer from the AM atom to the antibonding $2\pi^*$ orbital of CO, probably via the substrate. The adsorption energies of the coadsorbates have been observed to increase in calorimetric studies[3] and in thermal desorption experiments.[4]

According to our earlier results, the presence of K does not promote the CO dissociation on Co(0001) at room temperatures and at UHV conditions.[5] On the contrary, on polycrystalline Co foil, where CO dissociation has been seen,[6,7] the K atoms inhibit the CO dissociation probably by preferential adsorption at the same sites facilitating the C-O bond breaking.[8] The binding energies of both K and CO increase, however, as evidenced by the shift in the desorption maxima in thermal desorption (TDS) experiments[5] in accordance with CO and AM coadsorption on other transition metals. On Co foils a small increase in the production of longer chain hydrocarbons during CO hydrogenation at atmospheric pressures, normally explained by the increased tendency for CO dissociation, has been observed due to K promotion.[9] This effect is, however, much smaller than what is reported on the Ni surface.[10]

This paper is part of a larger study of adsorbate structures on Co(0001): The structures of the clean surface and the (2×2)-K (Refs. 11,12) and that of the $(\sqrt{3}\times\sqrt{3})R30°$-CO overlayer[13,14] have been reported earlier. The coadsorption of potassium and CO on Co(0001) has been studied in the past with TDS, low-energy electron diffraction (LEED), x-ray photoelectron spectroscopy (XPS) and low-energy ion scattering (LEIS). Based on these studies, we know that the adsorption takes place molecularly on the surface and the (2×2) structure is formed with one K atom and two CO molecules in the unit cell. The CO molecules are located between the K atoms so that the oxygen atoms are located closer to the surface than the K atoms.[5] In this paper we report the (2×2) surface structure formed during coadsorption of CO and K on Co(0001).

Coadsorption structures of CO and alkali metals have been solved only in the case of $c(2\times2)$-$(K+CO)$ on $Co(10\bar{1}0)$,[15] (2×2)-$(K+2CO)$ on Ni(111) (Ref. 16) and (2×2)-$(Cs+2CO)$ on Ru(0001).[17] The current results will be compared to these studies. In this respect we will discuss the CO bond lengths and the possible trends for CO dissociation on transition metal surfaces. A review has recently appeared discussing the existing coadsorption structures.[18]

We pose three questions for the alkali-metal coadsorption with CO: (i) What are the actual adsorption sites on the surface and how does this differ from the single absorbant case? (ii) How does the coadsorption affect the bond length of the CO molecule and the radius of the alkali metal and how do these correlate with the increased tendency of CO dissociation? (iii) How does the coadsorption change the binding of the adsorbed molecules to the surface and what is the mechanism causing this effect?

II. EXPERIMENT

The experiments were performed in a stainless steel UHV chamber with facilities for, e.g., x-ray photoelectron spectroscopy, thermal desorption spectroscopy, and low-energy

electron diffraction measurements. The system was pumped with an ion pump, and the base pressure during the experiments was around 50 nPa. A more detailed description of the UHV setup is available elsewhere.[5,19]

The Co(0001) sample disk was spot welded to the sample holder via tantalum wires, which were used both for resistive heating and conducting heat to the heat sink cooled with liquid nitrogen. The lowest attainable sample temperature of 160 K was used in the experiments. The manipulator stage could be rotated around the vertical axis and the sample holder provided azimuthal rotation enabling accurate alignment of the sample normal along the electron beam.

The initial cleaning procedure of the sample has been described earlier.[20] Between the experiments, the surface residues were removed by one hour sputtering with 1.1 keV Ar^+ ions, followed by annealing at 650 K for one to two hours. Cleanliness of the sample was checked by measuring the O 1 s and C 1s peaks using XPS before each measurement. The final test for the cleanliness was the formation of the LEED pattern of the $(\sqrt{3}\times\sqrt{3})R30°$ structure. This surface structure was obtained by exposing the Co(0001) crystal to 1.25 L of CO at 160 K, as described earlier by us.[14]

Potassium evaporation was accomplished with a standard SAES getter source at a distance of about 2 cm from the sample. A current of 4.6 A was passed through the getter, and four minutes was allowed for the stabilization of the K flux before each evaporation. The (2×2)-K structure was prepared by depositing a full monolayer of potassium at room temperature and subsequently heating the surface up to 400 K as reported earlier by us.[11,12]

When the (2×2)-K surface was exposed to CO, the quality of the LEED pattern improved, but no other changes were detected indicating formation of a (2×2)-(K+nCO) structure. A saturation exposure of 45 L of CO were used. The amount of CO in the coadsorption phase was deduced comparing the TDS spectra from the $(\sqrt{3}\times\sqrt{3})R30°$-CO and (2×2)-(K+2CO) structures, resulting in the structure where there is two CO molecules in the unit cell.[5]

The LEED experiments were made with a four-grid rear-view LEED unit. The diffraction images were recorded to a computer with a video camera having a resolution of 512 $\times$512 pixels and 256 grayscales. The same computer controlled the incident electron beam, allowing measurements of the intensity versus voltage curves. More details on the LEED measurement is available in Refs. 13,21.

The degree of damage due to the electron beam was estimated by comparing visually the spot sizes and the brightness of the background before and after the LEED measurement. No changes in the quality of the LEED pattern was detected, even after extended exposures of electron beam, in contrary to the very delicate $(\sqrt{3}\times\sqrt{3})R30°$-CO structure.

III. COMPUTATIONAL DETAILS

The spot intensities in the diffraction images were analyzed off line after the measurement with a homemade software producing the experimental I(E) (intensity vs. energy) curves. The shape of the measured spot area is circular and its size is adjusted to give a constant area in the *k* space. The intensity of the diffraction spot was calculated without any background subtraction to minimize the amount of noise in the IV spectra.

The theoretical I(E) spectra were calculated using the symmetrized automated tensor LEED package of Barbieri and Van Hove.[22] The phase shifts were calculated using the Barbieri–Van Hove phase-shift package.[22] We used ten phase shifts in the calculation.

The real part of the inner potential was varied in the *R*-factor analysis. The imaginary part of the inner potential had a constant value of -5 eV. Because of the limited convergence range of tensor LEED, we repeated the calculation of the reference structure for a large range of K-Co distances in steps of 0.3 Å and again at the final *R*-factor minima.

For the substrate Co layers, a Debye temperature of 385 K was used. For the outermost Co layer an enhanced vibration amplitude was used, being $\sqrt{2}$ times the root-mean-square amplitude in the substrate. The adsorbate atoms were treated as one composite layer and the rumpled substrate layer was treated as another composite layer.

The theoretical and experimental I(E) spectra were compared using the Pendry *R* factor.[23] The total energy range of the symmetrically inequivalent beams was 2250 eV, of which 870 eV for integer-order beams and 1380 eV for half-order beams.

The termination of the (0001) surface leads to two different domains, both exhibiting threefold symmetry. The experimental data is an average over these domains and the diffraction pattern has sixfold symmetry. Each experimental curve can thus be calculated as an average of six individual spots save for the (3/2, 1/2) beam, which is an average of 12 spots. In the calculations, both terminations have threefold symmetry but they are averaged using equal weight in order to reproduce the experimental data. Additionally, in some of the models, three coexisting adsorbate domains were formed, which were similarly averaged.

After obtaining the best-fit structure, the geometric parameters were varied one at a time in the neighborhood of the *R*-factor minimum and the uncertainties of the parameters were obtained using the variance of the *R* factor.

IV. RESULTS

The experimental intensity vs. energy curves for the three integer and five half-order beams are shown in Fig. 1 with solid lines.

The calculations were started by testing all high-symmetry sites for the K atom and the CO molecules in a rough search. The K atom can locate at the on-top site, fcc site, or hcp site and if the CO molecules are placed symmetrically between them, a combination of fcc and hcp sites, top and hcp sites, or top and fcc sites is obtained, respectively, as shown in Fig. 2. As an alternative, the CO molecules can be placed at the similar sites as the K atoms giving rise to rows of CO molecules between the K atoms and to the formation of three different adsorption domains rotated by 120°. As the last structure, the K atoms can be at the bridge sites, and the CO molecules at the top and fcc sites.

In each reference structure, the substrate was ideally ter-

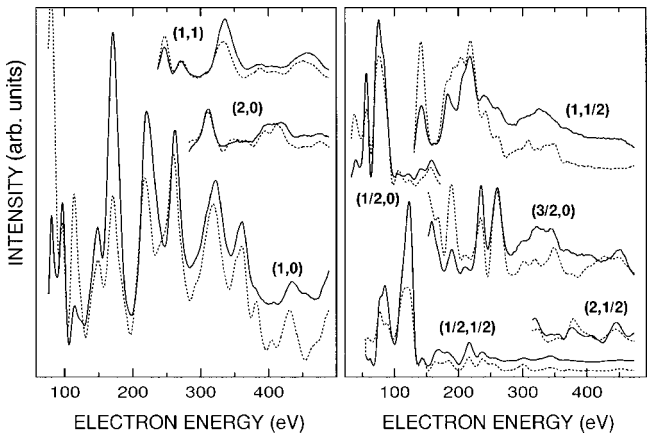

FIG. 1. Experimental (solid lines) and calculated (dashed lines) I(E) curves for the integer-order and half-order beams from the (2×2)-(K+2CO) structure on the Co(0001) surface.

minated. The distance from the potassium to the first Co layer was varied in 0.3 Å steps and the CO bond length was 1.13 Å. The reference structures were optimized with respect to the atomic positions of the K atom and the CO molecules, one Co layers, and the inner potential. The full data set of three integer-order and five half-order beams was used for the optimization. The Pendry *R* factors for the optimized

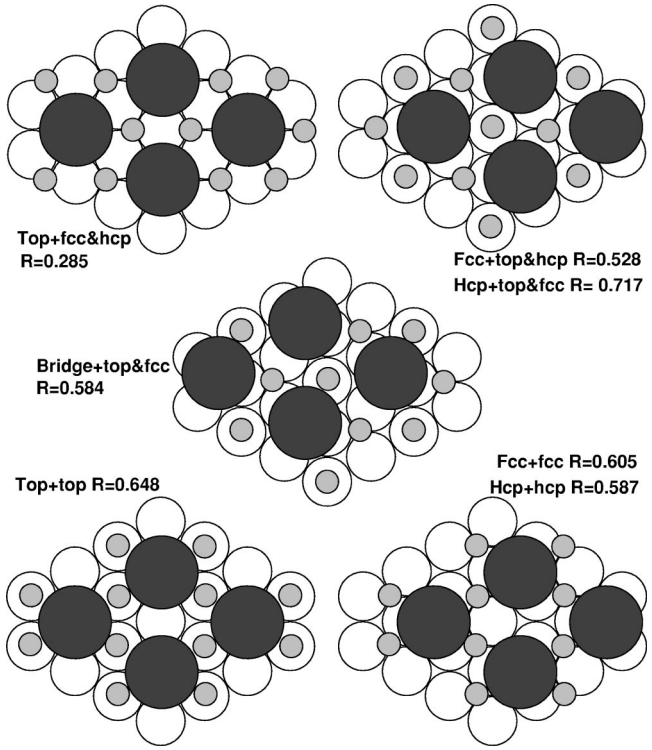

FIG. 2. Top views of the different (2×2)-(K+2CO) structures on the Co(0001) surface tested in the calculations. The white spheres are the surface Co atoms, the large black spheres are the K atoms, and the small gray spheres denote CO molecules standing perpendicular to the surface. Next to each structure are given the adsorption sites for the K atom and the two CO molecules in addition to the optimized Pendry *R*-factor values.

TABLE I. The final Pendry *R* factors for the different beams of the optimized (2×2)-(K+2CO) structure on Co(0001) shown in Fig. 3.

(1,0)	0.282
(1,1)	0.160
(2,0)	0.278
(1/2,0)	0.210
(3/2,0)	0.256
(1/2,1/2)	0.316
(1,1/2)	0.363
(2,1/2)	0.249
R_{tot}	0.273

structures after the rough search are given next to each structure in Fig 2. The top view cannot differentiate between the fcc and hcp sites, but the IV analysis gave different *R* factors for the K atoms at fcc sites compared to the K atoms at hcp sites, as shown with the two *R*-factor values adjacent to the right side structures in Fig 2.

The lowest Pendry *R* factor of 0.285, was obtained for the structure where the potassium atom is at the on-top site and the CO molecules at the hcp- and fcc-hollow sites. Based on the clearly higher *R* factors, the other adsorption site combinations were ruled out.

The K-Co distance was 3.03 Å and the fcc and hcp CO molecules were located so that the center of the O atoms are located 0.46 Å below the center of the K atom. A small difference in the bond length was detected between the CO molecules adsorbed on the fcc and hcp sites. This structure was then subjected to a refined analysis that also included variations of the nonstructural parameters.

As a result, we obtained three local minima for the K-Co distance: 3.14 Å ($R_P=0.273$), 2.66 Å ($R_P=0.342$), and 3.63 Å ($R_P=0.419$). The radius of the K atom calculated from these numbers are between the ionic and metallic radii of K, and can thus be regarded reasonable, but the differences in the *R*-factor values are large enough to exclude the two latter structures. The best-fit values of the *R* factors of the individual beams are shown in Table I. The best-fit intensity vs. energy curves for the three integer and five half-order beams are shown in Fig. 1 with dotted lines and can be compared to the experimental curves.

The final structure of the (2×2)-(K+2CO) layer on Co(0001) surface is presented in Fig. 3. The structure has a K-Co distance of 3.14 ± 0.05 Å. The C-Co layer distances for the fcc and hcp sites are 1.38 ± 0.11 Å and 1.32 ± 0.19 Å, giving C-Co bond lengths of 2.00 ± 0.08 Å, and 1.96 ± 0.13 Å, respectively. The layer distances of the oxygen atoms and the outermost Co layer are 2.58 ± 0.06 Å for the fcc site and 2.56 ± 0.07 Å for the hcp site. The C-O bond lengths, calculated from the positions of the C and O atoms, for the fcc and hcp sites, are 1.20 ± 0.13 Å and 1.24 ± 0.20 Å. The accuracy in the position of the carbon atom is rather low, but that for the oxygen atom is much better. This can result from the shadowed position of the rather weak scatterer of the carbon atom in the midst of other

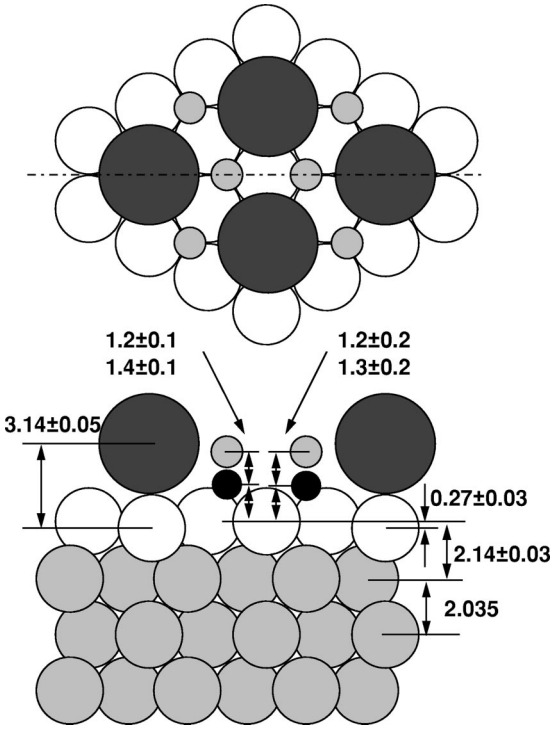

FIG. 3. Top view (upper panel) and side view cut along the $(11\bar{2}0)$ surface (lower panel) of the (2×2)-(K+2CO) structure on the Co(0001) surface. The white spheres denote the outermost Co atoms and the light gray spheres the Co atoms below the surface. The large black spheres are the K atoms and the small black and gray spheres are carbon and oxygen atoms, respectively. The length unit is 1 Å.

scatterers. The results also indicate huge buckling of 0.27 ± 0.03 Å in the top most Co layer, where the Co atom below K is pushed towards the bulk with respect to the three other surface atoms in the unit cell. The first Co-Co layer distance is 2.14 ± 0.03 Å and, thus, relaxed outwards from the bulk value of 2.035 Å. The final value of the Pendry *R* factor is 0.273.

The Debye temperatures of the adsorbed layer in the final analysis were optimized to 215 K for potassium, 425 K for carbon, and 445 K for oxygen. The optimum value of the inner potential is 7.4 eV with an imaginary part value of -5 eV.

V. DISCUSSION

Based on our earlier measurements of the K and CO adsorption and coadsorption, we know the following: *CO molecules adsorb* on the Co(0001) surface molecularly and form three different surface structures depending on the coverage and temperature, the most stable of which is the $(\sqrt{3}\times\sqrt{3})R30°$-CO seen below 330 K. The desorption from this phase takes place around 390 K.[14,24,25] The positions of the atoms on the surface have been analyzed with dynamical LEED technique and the results indicate CO adsorption on the on-top site.[13]

Adsorption of potassium on Co(0001) led to the formation of a (2×2)-K overlayer with coverage ranging from 0.18 to 0.31 at room temperature. The best quality LEED pattern was obtained with the optimum coverage of $\theta=0.25$. The desorption spectrum of the (2×2)-K overlayer was very broad and lacked a well-defined maximum typical for clean alkali metal on a transition metal surface.[11] The (2×2)-K structure has been analyzed with dynamical LEED technique and the results indicate K adsorption on the on-top site.[12]

When the (2×2)-K surface was exposed to CO, the symmetry of the LEED pattern remained the same, indicating a formation of (2×2)-(K+2CO) structure. In the TD spectra of the *coadsorption phase*, the K desorption took place in two distinct stages, around 430 and 570 K, and the CO desorption peak was shifted from 380 K seen in $(\sqrt{3}\times\sqrt{3})R30°$-CO to 570 K. The CO desorption was taking place simultaneously with the potassium desorption. The Monte Carlo simulation indicated an attractive interaction between K and CO and a repulsion between the neighboring K atoms.[5] With LEIS, the outmost surface layer was found to be composed of K and O atoms, indicating that those atoms were almost at the same elevation on the surface. These studies are now completed by the full structural analysis of the (2×2)-(K+2CO) surface.

A summary of the structural parameters of the *alkali atom* during adsorption and coadsorption with CO on transition-metal surfaces is given in Table II. The Alkali atoms adsorb on the on-top site of the close-packed transition-metal surface in the case of (2×2)-K structures on, e.g., Co(0001) (Ref. 12) and Ni(111) (Refs. 26,27), as well as in the case of Cs on Ru(0001).[28] In the case of coadsorption of an alkali metal and CO, our results are in line with the other two known structures where the alkali atom resides at the on-top site.[16,17] However, in the system where the original adsorption site for the alkali metal is not the on-top site on a closed packed surface, such as the (2×2)-K on Pt(111),[29] a recent structural analysis indicated that the alkali atom in this case also remains in its original adsorption site in the coadsorption.[30]

The size of the alkali atom increases due to the coadsorption in all the cases given in Table II. The increase is larger with potassium than with cesium probably because of the larger initial size of the Cs atom. On Co$(10\bar{1}0)$, the change in the K radius is huge compared to the close-packed surfaces and clearly due to the fourfold coordination of the K atom, resulting in a large change in the bond length with a small increase in the elevation. The increase in the alkali-metal radius in coadsorption is against the conventional interpretation, where the alkali metal acts as an electron donor during CO adsorption and is expected to increase its degree of ionization and thus move closer to the surface. Both the charge transfer from the alkali atom to the CO molecule, seen in the density functional theory calculations,[31] and the increase in the AM radius should increase the dipole moment of the AM-surface complex and give rise to a decrease in the work function. Because the charge from AM is not left to the substrate but to the CO molecule, the dipole moment of the O-C-surface complex compensates the proposed decrease in the work function, and experimentally, the work function

TABLE II. Structural parameters of the alkali atom for the alkali adsorption and coadsorption with CO on transition metal surfaces. AM-*s* indicates the distance between the alkali atom and the nearest substrate atom. A negative value for the buckling means moving the substrate atom towards the bulk. Estimated errors are given in brackets in hundredths of Å . In the case of Co($10\bar{1}0$), the buckling is in the second Co layer.

Substrate	Structure	AM site	AM-*s* (Å)	AM radius (Å)	Buckling (Å)	Method	Ref.
Co(0001)	(2×2)-K	top	2.93(11)	1.68	−0.16(3)	LEED	12
Co(0001)	(2×2)-(K+2CO)	top	3.14(5)	1.89	−0.27(3)	LEED	this work
Ni(111)	(2×2)-K	top	2.82(4)	1.57	−0.12(2)	LEED	26
Ni(111)	(2×2)-K	top	2.87(3)	1.62	−0.01	PED	27
Ni(111)	(2×2)-(K+2CO)	top	3.02(3)	1.77		PED	16
Pt(111)	(2×2)-K	hcp	3.12(4)	1.74	−0.07(2)	LEED	29
Pt(111)	$(\sqrt{3}\times\sqrt{3})R30°$-(K+CO)	hcp	3.28(6)	1.9	n/a	LEED	30
Ru(0001)	(2×2)-Cs	top	3.25(8)	1.9	−0.10(4)	LEED	28
Ru(0001)	(2×2)-(Cs+2CO)	top	3.35(4)	2.0	−0.19(4)	LEED	17
Co($10\bar{1}0$)	c(2×2)-K	fourfold	3.12(5)	1.87	≤0.1	LEED	45
Co($10\bar{1}0$)	c(2×2)-(K+CO)	fourfold	3.51(11)	2.26	−0.05(9)	LEED	15

actually increases due to coadsorption, as seen with Cs+CO on Ru(0001).[32] According to Over, the increased AM-substrate distance is due to the electrostatic attraction between the charge densities of CO and the alkali metal.[18]

The buckling of the first layer increases due to CO coadsorption as compared to K adsorption, both on Co and Ru close-packed surfaces, and the well the alkali atom is creating is rather deep. The second layer spacing of the Co substrate, calculated from the three Co atom is 0.08 Å longer than that for the clean surface, and 0.09 Å longer than in the case of K adsorption. Together with the increased buckling in the first Co layer, this leads to the same distance of 1.85 Å between the downwards shifted Co atom and the second layer atoms. Thus, it seems that the increased buckling can be understood as moving the first layer towards the vacuum. The third layer spacing coincides with the clean surface value.

The *CO molecule* occupies the on-top site in the $(\sqrt{3}\times\sqrt{3})R30°$-CO structure on Co(0001),[13] Ru(0001),[33,34] Rh(111),[35] and Cu(111).[36] Other adsorption sites with the $(\sqrt{3}\times\sqrt{3})R30°$-CO structure include bridge sites on Ni(111) (Ref. 37) and fcc sites on Pd(111).[38,39] From these structures, the coadsorption of CO with AM has previously been studied only on the Ru(0001),[17] Ni(111),[16] and Pt(111) (Ref. 30) surfaces. The on-top adsorption site of CO, seen with $(\sqrt{3}\times\sqrt{3})R30°$ structure for $\theta=\frac{1}{3}$, changes on Ru(0001) and Ni(111) to the fcc and hcp sites of the (2×2) structure with $\theta=\frac{1}{2}$ or to the hcp sites of the $(\sqrt{3}\times\sqrt{3})R30°$-K+CO structure on Pt(111). The CO molecules seem to give their place to the much larger AM atoms. The change in the CO adsorption site on the Ni(111) surface from the bridge to the threefold hollow sites stem from the occupation of K atoms at the on-top site, leaving no symmetrical bridge sites for the CO molecules. It should also be noted that on Ni(111) in the $c(4\times2)$-2CO structure, the fcc and hcp sites are already occupied without the alkali metal.[16,40] The change in the adsorption site originates from the increased back donation from metal to CO due to the alkali adsorption.[18] At the threefold hollow site the charge transfer from the metal to the $2\pi^*$ orbital of CO is maximized, making this site favorable for CO. A summary of the structural parameters during CO adsorption and coadsorption with alkali atoms on transition-metal surfaces is given in Table III.

The length of the carbon-substrate bond was found to increase by 0.2 Å with the change in the adsorption site during coadsorption on Co(0001). This increase is in line with the observations made in other coadsorption systems, and on Ni(111) (Refs. 16,37) the same values have been measured.

The direction of the first layer buckling is outwards in the case of CO adsorption on closed-packed surfaces,[13] but inwards in the case of alkali adsorption as shown in Table II. The increased rumpling due to coadsorption can be due to the charge transfer to the CO molecule resulting in stronger bonding of the molecule to the surface and decreased Co-Co interaction in the top substrate layers.

Calculating the electrostatic interaction between point charges located at the adsorption sites for K, C, and O atoms on the surface, and summing over several neighboring points, their image charges, and a charged surface layer ensuring charge balance, a potential energy of −2 eV for both CO and K, was obtained when the charges were +1 e, −1.5 e, and 0.74 e for K, C, and O atoms, respectively. This calculation is, of course, an oversimplification of the interactions on the surface, because no structure in the charge distribution within an atom has been taken into account. However, the values for the atomic charges are reasonable, and the value of the potential energy relates well to the measured simultaneous desorption around 550 K seen from the

TABLE III. Structural parameters of the CO molecule for CO adsorption and coadsorption with alkali atoms on transition metal surfaces. C-*s* indicates the bond length between the carbon atom and the substrate atom. A positive value for the buckling means moving the substrate atom outwards. Estimated errors are given in brackets in hundredths of Å .

Substrate	Structure	CO site	C-s (Å)	C-O (Å)	AM-O (Å)	Buckling (Å)	Method	Ref.
Co(0001)	$(\sqrt{3}\times\sqrt{3})R30°$-CO	top	1.78(6)	1.17(6)		0.04(4)	LEED	13
Co(0001)	(2×2)-(K+2CO)	fcc, hcp	1.94/1.99	1.20/1.24	2.91	−0.27(3)	LEED	this work
Ni(111)	$(\sqrt{3}\times\sqrt{3})R30°$-CO	bridge	1.78(5)	1.13			PED	37
Ni(111)	$c(4\times2)$-2CO	fcc, hcp	1.95/1.92	1.22/1.18			PED	16
Ni(111)	(2×2)-(K+2CO)	fcc, hcp	1.92(5)	1.20(7)	2.92		PED	16
Pt(111)	$(\sqrt{3}\times\sqrt{3})R30°$-CO	top	1.91(1)				ARPEFS	36
Pt(111)	$c(4\times2)$-2CO	top, br.	1.85(10)	1.15(5)			LEED	46
Pt(111)	$(\sqrt{3}\times\sqrt{3})R30°$-(K+CO)	hcp	2.08(6)	1.26(6)	2.87	n/a	LEED	30
Ru(0001)	$(\sqrt{3}\times\sqrt{3})R30°$-CO	top	1.93(4)	1.10(5)		0.07(3)	LEED	34
Ru(0001)	(2×2)-(Cs+2CO)	fcc, hcp	2.18(4)	1.10(5)	3.16	-0.19(4)	LEED	17
Co($10\bar{1}0$)	$p(2\times1)$-CO	top					RAIRS	41
Co($10\bar{1}0$)	c(2×2)-(K+CO)	bridge	1.90	1.20(8)	2.87		LEED	15

(2×2)-(K+2CO) structure. The mutual stabilization of CO and alkali metal has been observed with the other systems as well, and explained by the electrostatic interaction between $AM^{+\delta}$ and $CO^{-\epsilon}$ ions.[18]

Unfortunately, there is no structural study of CO adsorption on Co($10\bar{1}0$). Reflection-absorption infrared spectroscopy, however, indicated top-site adsorption for $p(2\times1)$ structure with coverage $\theta<0.5$ based on the CO stretch of 1994 cm^{-1},[41] although assignment of the adsorption site based on vibrational data is uncertain, especially at higher coverage.[35,42,43] The adsorption site thus changes from the assumed on-top site to the center of gravity of the K atoms, giving a short bridge site displaced by 0.5 Å towards the neighboring atomic row. The stretch frequency of the CO molecule in the c(2×2)-(K+CO) structure shifts to 1732 cm^{-1}, which is lower than the value expected for bridge or threefold coordinated CO on clean surface. However, the authors were expecting an even more pronounced decrease in the stretch frequency due to the short range attractive interaction between K and O.[44]

The optimum C-O bond length increases from the value of 1.17 ± 0.06 Å seen with CO only[13] to 1.20 ± 0.11 Å and 1.24 ± 0.19 Å for the fcc or hcp sites and they are clearly longer than the gas phase value of 1.13 Å. Because the error margins in the C-O bond lengths are quite large, the hcp and fcc sites can be regarded similarly on Co(0001). The general effect due to AM coadsorption is an increase in the CO bond length as seen in Table III. This can be taken to indicate the tendency of AM to enhance the dissociation CO on transition-metal surfaces.

The promotion effect of K in CO hydrogenation on Co and Ni surfaces can be partially explained as an increased bond length of the CO molecule. On clean metals, the selectivity towards methane is higher on Ni than on Co, and K deposition on the surface produces a more pronounced effect on Ni. On clean Co(0001), the C-O bond length is longer than on Ni(111), but after K addition almost equal bond lengths have been measured.

VI. CONCLUSIONS

In this paper we have presented a quantitative structural analysis of the (2×2)-(K+2CO) structure on Co(0001) surface using low-energy electron diffraction together with dynamical LEED calculations. The potassium atom adsorbs on the top site as was the case with the (2×2)-K structure. The bond length increases by 0.2 Å to 3.14 ± 0.05 Å.

The CO molecules are shifted from the top sites of the $(\sqrt{3}\times\sqrt{3})R30°$-CO structure to the threefold hollow fcc and hcp sites. The molecular axis is still perpendicular to the surface with the carbon atom bonding to the three Co atoms. The CO bond lengths are 1.20 ± 0.11 Å and 1.24 ± 0.19 Å, and the Co-C distances 1.94 and 1.99 Å for the CO molecules at the fcc and hcp sites, respectively. The first Co layer distance undergoes huge buckling where the Co atom underneath the K atom are pushed 0.27 ± 0.03 Å towards the bulk.

ACKNOWLEDGMENTS

This work was supported by the Academy of Finland and the Neste Foundations.

*Corresponding author: Jouko.Lahtinen@hut.fi
†Current address: VTT Building Technology, Fire Technology, P.O. Box 1803, 02044 VTT, Finland.
‡Current address: Picker Nordstar Inc., P.O. Box 185, 01511 Vantaa, Finland.

[1] J. C. Campuzano, *The Adsorption of CO by the Transition Metals*, Vol. 3, in *The Chemical Physics of Solid Surfaces and Heterogeneous Catalysis*, edited by D. A. King and D. P. Woodruff (Elsevier, New York, 1990).
[2] M. Kiskinova, *New Trends in CO Activation*, Vol 64, in *Studies in Surface Science and Catalysis*, edited by L. Guczi (Elsevier, New York, 1991).
[3] N. Al-Sarraf, J. T. Stuckless, C. E. Wartnaby, and D. A. King, Surf. Sci. **283**, 427 (1993).
[4] H. Bonzel, Surf. Sci. Rep. **8**, 43 (1987).
[5] J. Vaari, J. Lahtinen, T. Vaara, and P. Hautojärvi, Surf. Sci. **346**, 1 (1996).
[6] J. Nakamura, I. Toyoshima, and K. Tanaka, Surf. Sci. **201**, 185 (1988).
[7] U. Bardi, P. Tiscione, and G. Rovida, Appl. Surf. Sci. **127**, 299 (1986).
[8] J. Vaari, J. Lahtinen, and P. Hautojärvi, Appl. Surf. Sci. **78**, 255 (1994).
[9] J. Lahtinen and G. A. Somorjai, J. Mol. Catal. A: Chem. **130**, 255 (1996).
[10] C. T. Campbell and D. W. Goodman, Surf. Sci. **123**, 413 (1982).
[11] T. Vaara, J. Vaari, and J. Lahtinen, Surf. Sci. **395**, 88 (1998).
[12] J. Lahtinen, J. Vaari, T. Vaara, P. Kaukasoina, and M. Lindroos, Surf. Sci. **425**, 90 (1999).
[13] J. Lahtinen, J. Vaari, K. Kauraala, E. A. Soares, and M. A. Van Hove, Surf. Sci. **448**, 269 (2000).
[14] J. Lahtinen, J. Vaari, and K. Kauraala, Surf. Sci. **418**, 502 (1998).
[15] P. Kaukasoina, M. Lindroos, P. Hu, D. A. King, and C. J. Barnes, Phys. Rev. B **51**, 17 063 (1995).
[16] R. Davis, R. Toomes, D. P. Woodruff, O. Schaff, V. Fernandez, K.-M. Schindler, K.-U. Weiss, R. Dippel, V. Fritsche, and A. M. Bradshaw, Surf. Sci. **393**, 12 (1997).
[17] H. Over, H. Bludau, R. Kose, and G. Ertl, Surf. Sci. **331–333**, 62 (1995).
[18] H. Over, Prog. Surf. Sci. **58**, 249 (1998).
[19] J. Vaari, Ph.D. thesis, Helsinki University of Technology, 1995.
[20] J. Lahtinen, J. Vaari, A. Talo, A. Vehanen, and P. Hautojärvi, Surf. Sci. **245**, 244 (1991).
[21] T. Vaara, Ph.D. thesis, Helsinki University of Technology, 1997.
[22] A. Barbieri and M. A. Van Hove, httl://electron.lbl
[23] J. B. Pendry, J. Phys. C **13**, 937 (1980).
[24] M. E. Bridge, C. M. Comrie, and R. M. Lambert, Surf. Sci. **67**, 393 (1977).
[25] H. Papp, Surf. Sci. **129**, 205 (1983).
[26] P. Kaukasoina, M. Lindroos, R. D. Diehl, D. Fisher, S. Chandavarkar, and I. R. Collins, J. Phys.: Condens. Matter **5**, 2875 (1993).
[27] R. Davis, X.-M. Hu, D. P. Woodruff, K.-U. Weiss, R. Dippel, K.-M. Schindler, Ph. Hoffmann, V. Fritsche, and A. M. Bradshaw, Surf. Sci. **307–309**, 632 (1994).
[28] H. Over, H. Bludau, M. Skottke-Klein, G. Ertl, W. Moritz, and C. T. Campbell, Phys. Rev. B **45**, 8638 (1992).
[29] S. More, W. Berndt, A. M. Bradshaw, and R. Stumpf, Phys. Rev. B **57**, 9246 (1998).
[30] S. D. More, Ph.D. thesis, FU-Berlin, 1998.
[31] A. P. Seitsonen, Ph.D. thesis, Berlin University of Technology, 2000.
[32] S. Fichtner-Endruschat, V. De Renzi, A. Morgante, S. Schwegmann, H. Bludau, R. Schuster, A. Bottcher, and H. Over, J. Chem. Phys. **108**, 774 (1998).
[33] G. Michalk, W. Moritz, H. Pfnür, and D. Menzel, Surf. Sci. **129**, 92 (1983).
[34] H. Over, W. Moritz, and G. Ertl, Phys. Rev. Lett. **70**, 315 (1993).
[35] M. Gierer, A. Barbieri, M. A. Van Hove, and G. A. Somorjai, Surf. Sci. **391**, 176 (1997).
[36] E. J. Moler, S. A. Kellar, W. R. A. Huff, and Z. Hussain, Phys. Rev. B **54**, 10 862 (1996).
[37] S. D. Kevan, R. F. Davis, D. H. Rosenblatt, J. G. Tobin, M. G. Mason, D. A. Shirley, C. H. Li, and S. Y. Tong, Phys. Rev. Lett. **46**, 1629 (1981).
[38] H. Ohtani, M. A. Van Hove, and G. A. Somorjai, Surf. Sci. **187**, 372 (1987).
[39] T. Giessel, O. Schaff, C. J. Hirschmugl, V. Fernandez, K.-M. Schindler, A. Theobald, S. Bao, R. Lindsay, W. Berndt, A. M. Bradshaw, C. Baddeley, A. F. Lee, R. M. Lambert, and D. P. Woodruff, Surf. Sci. **406**, 90 (1998).
[40] L. D. Mapledoram, M. P. Bessent, A. Wander, and D. A. King, Chem. Phys. Lett. **228**, 527 (1994).
[41] R. L. Toomes and D. A. King, Surf. Sci. **349**, 1 (1996).
[42] D. Loffreda, D. Simon, and P. Sautet, Surf. Sci. **425**, 68 (1999).
[43] N. Materer, A. Barbieri, U. Starke, J. D. Batteas, M. A. Van Hove, and G. A. Somorjai, Phys. Rev. B **48**, 2859 (1993).
[44] R. L. Toomes and D. A. King, Surf. Sci. **349**, 19 (1996).
[45] C. J. Barnes, P. Hu, M. Lindroos, and D. A. King, Surf. Sci. **251/252**, 561 (1991).
[46] D. F. Ogletree, M. A. Van Hove, and G. A. Somorjai, Surf. Sci. **173**, 351 (1986).